it to also be present in the δ phase.

Finally, it should be recognized that in this structure there is a clear violation of the equivalency postulate,[28] since the asymmetric unit of structure contains two chemically identical monomer units which have different conformations (TT vs. TG).

Conclusions

The structure of the γ phase of PVF_2 has been determined. The unit cell is orthorhombic with dimensions $a = 0.497$, $b = 0.966$, and $c = 0.918$ nm. The chain conformation is approximately TTTGTTTG'. Individual chains have a net electrical dipole, and the chain packing is such that the unit cell is polar. The chains pack in a statistical parallel–antiparallel manner. The statistical nature of the structure can be modeled with a hypothetical four-chain unit cell belonging to space group $C2cm$. The residuals for this structure are $R' = 0.174$ and $R'' = 0.253$.

Acknowledgment. This research was supported by the Defense Advanced Research Projects Agency and monitored by the Army Night Vision Laboratory under Contract No. DAAK 70-77-C-0055.

References and Notes

(1) J. B. Lando, H. G. Olf, and A. Peterlin, *J. Polym. Sci., Part A-1*, **4**, 941 (1966).
(2) W. M. Prest, Jr., and D. J. Luca, *J. Appl. Phys.*, **46** (10), 4136 (1975).
(3) R. Hasegawa, Y. Takahashi, Y. Chatani, and H. Tadokoro, *Polym. J.*, **3** (5), 600 (1972).
(4) W. W. Doll and J. B. Lando, *J. Macromol. Sci., Phys.*, **B4** (2), 309 (1970).
(5) G. T. Davis, J. E. McKinney, M. G. Broadhurst, and S. C. Roth, *J. Appl. Phys.*, **49** (10), 4998 (1978).
(6) D. Naegele, D. Y. Yoon, and M. G. Broadhurst, *Macromolecules*, **11** (6), 1297 (1978).
(7) G. R. Davies and H. Singh, *Polymer*, **20**, 772 (1979).
(8) R. Hasegawa, M. Kobayashi, and H. Tadokoro, *Polym. J.*, **3** (5), 591 (1972).
(9) W. W. Doll and J. B. Lando, *J. Macromol. Sci., Phys.*, **B2** (2), 219 (1968).
(10) W. M. Prest, Jr., and D. J. Luca, *J. Appl. Phys.*, **49** (10), 5042 (1978).
(11) S. Osaki and Y. Ishida, *J. Polym. Sci., Polym. Phys. Ed.*, **13**, 1071 (1975).
(12) A. J. Lovinger and H. D. Keith, *Macromolecules*, **12** (5), 919 (1979).
(13) G. Cortilli and G. Zerbi, *Spectrochim. Acta, Part A*, **23**, 2216 (1967).
(14) Ye. L. Gal'Perin, B. P. Kosmynin, and R. A. Bychkov, *Vysokomol. Soedin., Ser. B*, **12**, 555 (1970).
(15) M. Kobayashi, K. Tashahiro, and H. Tadokoro, *Macromolecules*, **8**, 158 (1975).
(16) S. Weinhold, M. H. Litt, and J. B. Lando, *J. Polym. Sci., Polym. Lett. Ed.*, **17**, 585 (1979).
(17) M. A. Bachmann, W. L. Gordon, J. L. Koenig, and J. B. Lando, *J. Appl. Phys.*, **50** (10), 6016 (1979).
(18) S. K. Tripathy, R. Potenzone, Jr., A. J. Hopfinger, N. C. Banik, and P. L. Taylor, *Macromolecules*, **12**, 656 (1979).
(19) N. C. Banik, P. L. Taylor, S. K. Tripathy, and A. J. Hopfinger, *Macromolecules*, **12**, 1015 (1979).
(20) M. H. Litt, S. Mitra, and J. B. Lando, to be submitted to *Macromolecules*.
(21) G. J. Welch, *Polymer*, **15**, 429 (1974).
(22) P. J. C. Smith and S. Arnott, *Acta Crystallogr., Sect. A*, **34**, 3 (1978).
(23) "International Tables for X-Ray Crystallography", Vol. 1, Kynoch Press, Birmingham, England, 1952, p 126.
(24) W. W. Doll and J. B. Lando, *J. Macromol. Sci., Phys.*, **B4** (4), 889 (1970).
(25) K. Matsushige and T. Takemura, *J. Polym. Sci., Polym. Phys. Ed.*, **16**, 921 (1978).
(26) K. Matsushige, K. Nagata, and T. Takemura, *Jpn. J. Appl. Phys.*, **17** (3), 467 (1978).
(27) J. Scheinbeim, C. Nakafuku, B. A. Newman, and K. D. Pae, *J. Appl. Phys.*, **50** (6), 4399 (1979).
(28) G. Natta and P. Corradini, *Nuovo Cimento, Suppl.*, **15**, 9 (1960).

Packing Analysis of Carbohydrates and Polysaccharides. 11. Molecular and Crystal Structure of Native Ramie Cellulose

Carrie Woodcock and Anatole Sarko*

Department of Chemistry, State University of New York, College of Environmental Science and Forestry, Syracuse, New York 13210. *Received January 9, 1980*

ABSTRACT: The crystal structure of ramie cellulose I has been determined by an X-ray diffraction analysis combined with stereochemical model refinement. The structure crystallizes in a monoclinic, two-chain unit cell, in which the chain arrangement is parallel and the most likely space group is $P2_1$. The conformation of both chains is based on a one glucose residue asymmetric unit, with the hydroxymethyl group tg, and the 2_1 screw axis coincident with the chain axis. The chains are hydrogen bonded two dimensionally into sheets arranged along the (200) planes. The sheets are staggered by $^1/_4c$ relative to one another and have no hydrogen bonds between them. In these features, the crystal structures of ramie and *Valonia* cellulose are nearly identical. The X-ray reliability index $R'' = 0.194$, and the parallel-chain structure is statistically preferred over the best antiparallel structure at a 99.5% significance level.

Previous crystallographic studies of cellulose I of the alga *Valonia ventricosa* have shown that this highly crystalline native cellulose has a parallel-chain structure.[2,3] Other native celluloses, typically those of ramie, cotton, or wood, are, however, less crystalline and may have a unit cell smaller than that of *Valonia* cellulose.[4] As a result, a belief persists that not all native celluloses are identical in crystal structure and that some may be based on an antiparallel-chain lattice. The present study on ramie cellulose was, therefore, undertaken to determine its crystal structure in suitable detail for a comparison with the *Valonia* cellulose. In view of the apparent identity of the diffraction patterns of ramie and similar celluloses, this study should also have a bearing on the structure of other native celluloses.

Experimental Procedures

A sample of purified, relatively high crystalline ramie was obtained from Dr. T. E. Timell of this college. The sample was treated with the cellulase of *Pestalotiopsis westerdijkii* QM381 (obtained from Dr. M. Mandels, U.S. Army Natick Research and Development Command, Natick, Mass.) at the optimum conditions for this enzyme[5] in an effort to improve crystallinity further. However, no significant improvement in the resolution of the X-ray diffraction diagrams resulted, except that the faint layer-line

0024-9297/80/2213-1183$01.00/0

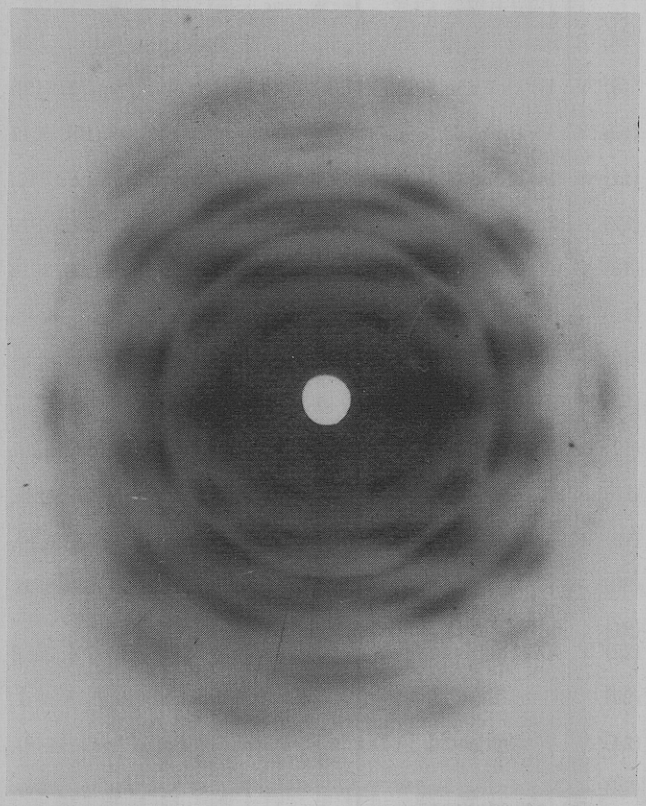

Figure 1. Flat-film X-ray diffraction diagram of ramie cellulose I. The fiber axis is vertical.

streaks usually present in the X-ray diagrams of native celluloses were eliminated.

The X-ray diffraction diagrams were recorded with nickel-filtered Cu Kα radiation (λ = 1.5418 Å) on multiple-sheet packs of Ilford Type G industrial X-ray film in an evacuated, flat-film pinhole camera equipped with 0.025-in.-diameter pinholes. A typical diffraction diagram is shown in Figure 1.

Twenty-nine reflections, on six layer lines, were sufficiently well resolved for the unit cell determination. The parameters of the Meyer and Misch unit cell were used to index these reflections, followed by least-squares refinement of the parameters against the measured d spacings.

The relative intensities of the reflections were determined from layer-line scans recorded with a Joyce-Loebl microdensitometer. The recorded intensity envelopes on five layer lines (equator and four higher layers) were resolved with a least-squares curve resolution computer program into 35 individual intensities, corresponding to visually observed reflections. A total of 100 reflections were predicted to contribute to these 35 intensities by calculation from the unit cell parameters. In addition, 15 predicted, but not observed, reflections were assigned half of the minimum observable intensity.

The set of intensities were corrected for Lorentz and polarization factors,[7] reflection arcing,[7] distance of diffracted ray to film, Franklin artificial temperature factor,[8] and film scanning direction other than radial. The coefficient a of the Franklin artificial temperature factor was set equal to 0.80 by a procedure explained in ref 1. The square roots of the corrected, relative integrated intensities constituted the observed structure factor amplitudes.

Methods of Refinement

The procedures and strategy of crystal structure analysis of celluloses followed in this study have been previously described.[9,10] The initial chain model was constructed with the atomic coordinates of *Valonia* cellulose and with a twofold screw axis coincident with the chain axis.[2] The two chains traversing the unit cell were placed at the corner and center of the a–b plane of the cell, respectively, either with parallel or antiparallel packing polarity. The refinement of the resulting two models was started from different rotational and translational positions of the chains, as well as from different rotational positions of the hydroxymethyl group. In the refinement, both conformation and packing of the chains were simultaneously optimized by minimizing the function

$$Y = \sum_{i=1}^{l}\left(\frac{r_i - r_{0i}}{\mathrm{SD}_i^r}\right)^2 + \sum_{i=1}^{m}\left(\frac{\theta_i - \theta_{0i}}{\mathrm{SD}_i^\theta}\right)^2 + \sum_{i=1}^{n}\left(\frac{\phi_i - \phi_{0i}}{\mathrm{SD}_i^\phi}\right)^2 + \frac{1}{W^2}\sum_{\substack{i=1\\j=1}}^{N} w_{ij}(d_{ij} - d_{0ij})^2 \quad (1)$$

where r_i are the bond lengths, θ_i are the bond angles, ϕ_i are the conformational (torsion) angles, and r_{0i}, θ_{0i}, and ϕ_{0i} are the corresponding standard values[11] with SD_i standard deviations.[11] The first three terms, therefore, minimize the strain in bond lengths, bond angles, and conformational angles during refinement. The last term, where d_{ij} is the contact distance between nonbonded atoms i and j and where d_{0ij} and w_{ij} are the corresponding equilibrium distance and weight of the interaction, respectively, minimizes the nonbonded repulsion energy.[12] The weighting factor W^{-2} is the weight of the nonbonded contact term in the entire function. The refinable variable parameters included all bond lengths, bond angles, and conformational angles of the asymmetric residue, as well as the chain-positioning parameters.

The models resulting from the stereochemical refinement were further refined against the observed structure factor amplitudes, with the residual R as the refinement criterion (eq 2). The best

$$R = \sum||F_o| - |F_c||/\sum|F_o| \quad (2)$$

models resulting from the first cycle of refinement were then rerefined against the X-ray data, but with stereochemical constraints imposed on the variable parameters and nonbonded contacts in order to guard against the development of unacceptable stereochemical features in the model. The refinement proceeded by minimizing the function

$$\Phi = fR'' + (1 - f)Y \quad (3)$$

where Y was the stereochemical function of eq 1 and R'' (multiplied by 100) was the weighted X-ray residual

$$R'' = \left[\frac{\sum_{m=1}^{M} w_m||F_o| - |F_c||_m^2}{\sum_{m=1}^{M} w_m|F_o|_m^2}\right]^{1/2} \quad (4)$$

used because the unobserved intensities were now included at half the weight. The weighting factor f in eq 3 was set at 0.8 to weight the R'' term slightly more than the Y term.

The variable parameters in both stages of X-ray refinement included the chain-positioning parameters, all conformational angles, and selected bond angles but not the bond lengths. In the final cycle of refinement, the components B_x, B_y, and B_z of an anisotropic temperature factor

$$B = \frac{h^2a^{*2}B_x}{4} + \frac{k^2b^{*2}B_y}{4} + \frac{l^2c^{*2}B_z}{4} \quad (5)$$

were included as refinable parameters. (In this equation, h, k, and l are reflection indices and a^*, b^*, and c^* are the reciprocal lengths of the unit cell axes.)

Results and Discussion

Unit Cell. The refinement of the unit cell parameters with the 29 reflections shown in Table I resulted in a monoclinic cell having dimensions a = 7.78 Å, b = 8.20 Å, c (fiber axis) = 10.34 Å, and γ = 96.5°. These parameters agree well with those previously determined by Meyer and Misch,[6] by Wellard,[13] and by Hebert and Muller in an electron diffraction study.[14] The observed and calculated d spacings are in good agreement, as shown in Table I. The calculated density, ρ_c = 1.64 g/cm^3, assuming four glucose residues and no water in the cell, is in reasonable agreement with the experimental density, ρ_e = 1.57 g/cm^3.

The three reflections present in the X-ray diffractogram of *Valonia* cellulose that required the large, eight-chain unit cell were absent in the X-ray diffractogram of ramie cellulose. (These reflections occurred at d = 8.61 and 4.42 Å on the first layer and d = 3.29 Å on the third layer.[2]) Because of the good quality of the X-ray diffraction pat-

Table I
Observed d Spacings Used in the Refinement of the Unit Cell

Miller indices hkl	d spacing, Å		
	obsd	predicted	difference
$\bar{1}10$	6.01	5.96	0.05
110	5.31	5.32	−0.01
200	3.90	3.87	0.03
040	2.04	2.04	0.00
400, 410	1.93	1.93	0.00
011	6.41	6.40	0.01
111	4.71	4.73	−0.02
201	3.61	3.62	−0.01
031	2.62	2.63	−0.01
$\underline{1}31$	2.42	2.41	0.01
$\bar{2}31$	2.29	2.29	0.00
002	5.15	5.17	−0.02
$\underline{0}12$	4.35	4.37	−0.02
$\bar{1}22$	3.06	3.05	0.01
122	2.85	2.87	−0.02
$\underline{0}32$	2.40	2.40	0.00
$\bar{2}32$	2.14	2.14	0.00
042, $\bar{1}42$	1.89	1.90, 1.89	−0.01, 0.00
013	3.20	3.17	0.03
113	2.92	2.89	0.03
023	2.64	2.63	0.01
033	2.13	2.13	0.00
133	2.02	2.01	0.01
114	2.34	2.33	0.01
$\underline{0}24$	2.17	2.18	−0.01
$\bar{1}34$, 224	1.86	1.85	0.01
134	1.78	1.79	−0.01
125	1.77	1.77	0.00
035	1.65	1.65	0.00

terns of ramie, these reflections would have been visible had they been present. As a consequence, the eight-chain cell or the alternative, two-chain triclinic unit cell proposed for *Valonia* cellulose[2] was thought not to be present in ramie. This assessment is in agreement with Hebert and Muller, who also found different unit cells for ramie and *Valonia*.[14]

The generally accepted space group for cellulose I is $P2_1$.[2,3] However, the presence of very weak odd-order meridionals 001 and 003 in all cellulose I diffractograms argues against this assignment. In view of this, a firm assignment of the space group was not made, even though the initial construction of the chain models and all early cycles of refinement were done in accordance with $P2_1$ symmetry.

Packing Analysis. The stereochemical refinement of both parallel and antiparallel models resulted in four acceptable models, two within each chain polarity. The criteria of acceptability included the absence of short nonbonded contacts and the formation of hydrogen bonds with lengths 2.50–3.10 Å. The characteristics of the four models described in Table II (supplementary material) are marked by the now familiar tg rotational position for the O_6 atom in at least one chain of the unit cell and a two-directional, intra- and intermolecular hydrogen-bond system that binds the chains into sheets.[2,3] For both parallel and antiparallel packing polarities, the pure tg models, i.e., those in which the O_6 rotation was the same in both chains of the unit cell, were slightly favored over those in which the O_6 rotations differed for the two chains. However, neither packing polarity could be picked as the more probable one on the basis of this analysis.

All other models, i.e., those with the O_6 atom in gt or gg positions, were rejected because of higher packing energies and the presence of short nonbonded contacts. (The detailed descriptions of the rejected models can be found in ref 1.)

X-ray Refinement. All of the models resulting from the packing refinement, including the rejected ones, were subsequently refined against the X-ray structure factor amplitudes. After the initial round of this refinement, four best models, with minimally acceptable stereochemical features, again resulted. As shown in Table II, two of these models, the parallel tg and the antiparallel tg, resembled the corresponding best-packing models, whereas the parallel, independent O_6 rotation model did not. The antiparallel, independent O_6 rotation model was very similar to the antiparallel, pure tg model. The parallel, pure tg model was slightly, but not significantly, favored by R and R'' factors over all other models. At the same time, the independent O_6 rotation models were beginning to border on stereochemical unacceptability, as indicated by the relatively high PE values. After the same models were refined with stereochemical constraints, minimizing the function shown in eq 3, it became clear from the increasing X-ray residuals and PE values (cf. Table II) that no advantages resulted from independent O_6 rotations, and these models were dropped from further cycles of refinement. It was also becoming evident that the best parallel model remained slightly, but consistently, favored over the best antiparallel model.

The final cycle of refinement was marked by elimination of $P2_1$ symmetry and the inclusion of an anisotropic temperature factor of the form shown in eq 5. As a consequence of symmetry elimination, the cellobiose residue now became the asymmetric unit, which meant that the lengths of the virtual bonds of the individual glucose residues comprising the cellobiose residue (i.e., the lengths of the vectors connecting successive bridge oxygens) became variable during refinement. Under $P2_1$ symmetry, the length of the virtual bond of the glucose asymmetric unit had remained fixed at its most probable value of 5.45 Å.

The results of this final stage of refinement are shown in Table III, and it is clear that the parallel model is now substantially favored over the antiparallel model. If the structure analysis is treated as a one-dimensional hypothesis, i.e., parallel vs. antiparallel chains, then with 50 observations (reflections) and 23 variables (refined in the final stage of analysis), the difference in the R'' factors for the two structures is significant at the 99.5% level, or the probability is at least 200:1 that the crystal structure of ramie cellulose is parallel.[15] This result is also supported by a comparison of the best parallel and antiparallel structures with the corresponding models predicted from packing analysis (cf. Table II), which shows that the energy and R'' factor minima for the parallel structure are close to identical, whereas the same is not true for the antiparallel structure. Further comparing the characteristics of the individual glucose units of the repeating cellobiose residue—in terms of bridge angles, virtual bond lengths, ϕ and ψ conformation angles, O_6 rotation angles, and the lengths of hydrogen bonds—shows that the two glucose residues are essentially equivalent and are thus very close to being related by a 2_1 screw axis. Although this is not consistent with the presence of odd-order meridionals, the intensities of the latter are very weak, suggesting, as discussed below, that their presence may be caused by some disorder in the structure.

The atomic coordinates of the final parallel structure are given in Table IV (supplementary material). Two projections of the unit cell, complete with hydrogen bonds, are shown in Figure 2.

During the course of the final X-ray refinement, some other variants of parallel models were also tested. For example, the final parallel model of Table III is an "up"

Table III
Most Probable Parallel and Antiparallel Models after Final Refinement (Space Group $P1$)

	O_6 tg, parallel model	O_6 tg, antiparallel model
bridge angle 1,[a] deg	117.5	117.4
bridge angle 2,[a] deg	117.1	117.3
corner chain rotation, deg	40.4	39.5
center chain rotation, deg	38.4	140.0
center chain translation, Å	−2.60	1.73
O_6 rotation (residue 1), deg	179.5	−179.5
O_6 rotation (residue 2), deg	179.8	−179.4
virtual bond[b] (residue 1), Å	5.446	5.436
virtual bond (residue 2), Å	5.446	5.433
conformation angles ϕ, ψ,[c] deg		
residue 1	26.6, −27.2	25.4, −26.1
residue 2	25.8, −27.0	25.1, −26.0
packing energy	24.4	30.2
conformation energy[d]	29.1	29.9
intrachain hydrogen bonds, Å		
$O_3(2)$-$O_5(1)$	2.65	2.67
$O_3(1)$-$O_5(2)$	2.66	2.67
$O_2(2)$-$O_6(1)$	2.64	2.60
$O_2(1)$-$O_6(2)$	2.63	2.60
interchain hydrogen bonds, Å		
$O_3(1)$-$O_6(1)$	2.92	2.93
$O_3(2)$-$O_6(2)$	2.92	2.93
$O_3(3)$-$O_6(3)$	2.89	2.94
$O_3(4)$-$O_6(4)$	2.89	2.94
R (eq 2)	0.220	0.309
R'' (eq 4)	0.193	0.246
anisotropic temperature factor components		
B_x	0.0	0.0
B_y	0.1	2.5
B_z	8.0	7.1

[a] Angle 1 is between residues 1 and 2; angle 2 is between residues 2 and 1 (see Figure 2). [b] Length of the vector connecting successive bridge oxygens. [c] $\phi = 0°$ when the bond sequence H_1-C_1-O_4'-C_4' is cis; $\psi = 0°$ when the bond sequence C_1-O_4'-C_4'-H_4' is cis; a positive angle is for the far bond clockwise relative to the near bond. [d] Nonbonded term of eq 1, restricted to intrachain contacts.

chain structure, according to the definition of Gardner and Blackwell.[3] An all-"down" parallel structure is also possible and could be obtained from the "up" structure by inverting the cell and changing the monoclinic angle to its complement. In refinement, the "down" parallel model would not improve from $R = 0.336$ and was rejected.

Possible Forms of Disorder. As shown in Table V (supplementary material), the calculated and observed structure factor amplitudes are, generally, in good agreement for the parallel structure. A discrepancy is present in the meridionals, which, although quantitatively not usable in the refinement, can be compared qualitatively. As already stated, the odd-order meridionals are not predicted by the final structure. For the even-order meridionals, the agreement for 004 is very good, but for 002 it is poor. The reasons for this lack of agreement are not known, although a good case can be made for at least two forms of disorder. For example, the 002 meridional is sensitive to chain translation along the c axis. As shown in Tables II and III, a relatively wide range is possible for this parameter in the parallel-chain models, without significantly affecting other characteristics of the structure. A disorder in translation may, therefore, exist and may account for the stronger than calculated 002 meridional.

It is also possible that the center chain is conformationally slightly different from the corner chain. This is

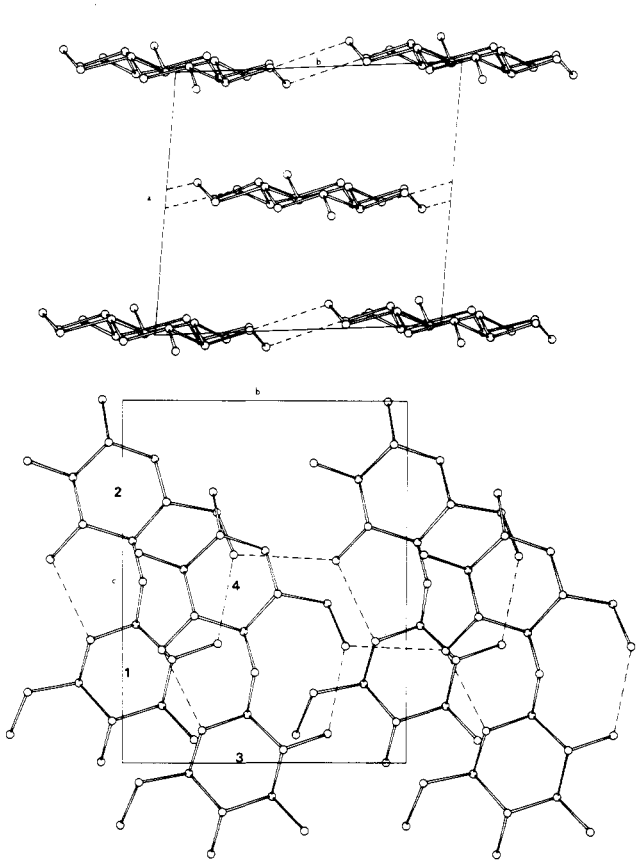

Figure 2. Unit cell projections of the parallel-chain structure of ramie cellulose I. Hydrogens are not shown; hydrogen bonds are indicated by dashed lines. Numbers 1 to 4 indicate residue numbering.

suggested by the slight differences in the chain rotation parameters for the two chains. Such a difference may also affect the translation of chains—in a more systematic manner than the disorder discussed above—possibly resulting in strengthening the 002 meridional.

Finally, the O_6 rotations may be slightly disordered, irrespective of disorder in the chain translation. This may not only affect the 002 meridional but will also result in the presence of weak odd-order meridionals.

Because of insufficient data, it was not possible to test for the presence of disorder. However, if good electron diffraction diagrams of ramie were available, containing more diffraction intensities, testing for these types of disorder could become possible.

Conclusions

The parallel-chain structure is clearly favored for ramie cellulose. In this respect, ramie and *Valonia* celluloses are identical. Further comparison of the two celluloses reveals other similar features. For example, the O_6 rotations are tg in both structures, and their hydrogen bond sequences are identical. However, there are some differences in their crystal structures. For example, although the neighboring sheets of chains are quarter-staggered relative to one another in both celluloses, it is probable, as suggested earlier,[16] that the stagger in the larger *Valonia* cell is more complicated, repeating in the a direction only after four sheets rather than two sheets as in the ramie unit cell. This would not alter the crystal structure significantly but would account for the different unit cell seen in *Valonia* cellulose.

The similarities between the two celluloses, however, appear to confirm the idea presented previously[2] that all native celluloses crystallize in the same manner because their biosynthetic mechanisms are likely to be the same

in all organisms. The similar X-ray diffraction diagrams of ramie and other fibrous celluloses support this. The subtle differences in the structures of different celluloses may, however, never be fully characterized. The only hope lies in the refinement with electron diffraction data, provided that a significant increase in the amount of data can be realized.

Acknowledgment. This work has been supported by the National Science Foundation (Grant No. CHE7727749).

Supplementary Material Available: Tables II (most probable models after initial cycles of refinement for space group $P2_1$), IV (Cartesian atomic coordinates of the parallel structure), and V (comparison of observed and calculated structure factors for the parallel structure) (10 pages). Ordering information is given on any current masthead page.

References and Notes

(1) C. Woodcock, M.S. Thesis, SUNY College of Environmental Science and Forestry, Syracuse, N.Y., 1979.
(2) A. Sarko and R. Muggli, *Macromolecules*, **7**, 486–94 (1974).
(3) K. H. Gardner and J. Blackwell, *Biopolymers*, **13**, 1975–2001 (1974).
(4) R. H. Marchessault and A. Sarko, *Adv. Carbohydr. Chem.*, **22**, 421–82 (1967).
(5) M. Mandels, personal communication. See also: M. Mandels and E. T. Reese, *Dev. Ind. Microbiol.*, **5**, 5–20 (1964).
(6) K. H. Meyer and L. Misch, *Helv. Chim. Acta*, **20**, 232–44 (1937).
(7) R. J. Cella, B. Lee, and R. E. Hughes, *Acta Crystallogr., Sect. A*, **26**, 118–24 (1970).
(8) R. E. Franklin and R. G. Gosling, *Acta Crystallogr.*, **6**, 678–85 (1953).
(9) A. J. Stipanovic and A. Sarko, *Macromolecules*, **9**, 851–7 (1976).
(10) A. Sarko, J. Southwick, and J. Hayashi, *Macromolecules*, **9**, 857–63 (1976).
(11) S. Arnott and W. E. Scott, *J. Chem. Soc., Perkin Trans. 2*, 324–35 (1972).
(12) P. Zugenmaier and A. Sarko, *Acta Crystallogr., Sect. B*, **28**, 3158–66 (1972).
(13) H. J. Wellard, *J. Polym. Sci.*, **13**, 471–6 (1954).
(14) J. J. Hebert and L. L. Muller, *J. Appl. Polym. Sci.*, **18**, 3373–7 (1974).
(15) W. C. Hamilton, *Acta Crystallogr.*, **18**, 502–10 (1965).
(16) A. Sarko, *Tappi*, **61**, 59–61 (1978).

Orientation Mode of Crystallites and Rodlike Texture of Polyethylene Crystallized from a Stressed Polymer Melt[1a]

Masaru Matsuo,*[1b] Fumihiko Ozaki,[1c] Hozumi Kurita,[1c] Shunji Sugawara,[1c] and Tetsuya Ogita[1c]

Department of Textile Engineering, Faculty of Home Economics, Nara Women's University, Nara 630, Japan, and Department of Textile Engineering, Faculty of Engineering, Yamagata University, Yonezawa 992, Japan. *Received October 13, 1978*

ABSTRACT: The orientations of the crystallites and of the rodlike texture of polyethylene crystallized from a shear-stressed polymer melt are investigated by means of X-ray diffraction and light scattering measurements in terms of the orientation distribution function. The rotation of the crystallite around its own *c* axis and the rotation of the rodlike texture around its own rod axis are both found to be restricted. As for the crystallites, the possibility of the existence of crystal *a* axes is most probable in the plane consisting of crystal *c* axes and the machine direction. As for the rodlike textures, the existence of rod axes is also most probable in the plane consisting of the crystal *c* axes and the machine direction. According to both distribution functions, the structure of the rodlike texture is postulated not to be cylindrical but rather to be platelike. The mechanical anisotropy of this specimen is hardly affected by the orientation of the crystal *c* axes. Young's modulus E and the storage modulus E' at 50 Hz do not decrease monotonically with increasing angle between the direction of external mechanical excitation and the machine direction, although the orientation distribution function of crystal *c* axes shows a monotonic curve having a maximum in the machine direction.

It is common knowledge that a polymer film crystallized from a shear-stressed polymer melt has a particular morphology with respect to the molecular and lamellar orientations. This arises from the crystallization conditions and varies with the type of polymer.[2-20] Detailed study of this morphology is important in investigating the mechanism of crystallization in melt spinning. There have been a number of papers on the morphology and crystallization of specimens crystallized from stressed polymer melts and solutions. Pennings et al.[7] reported that polyethylene crystallized from stirred solutions produces fibrous crystals termed row-nucleated shish-kebab structures by Keller et al.[2] on the basis of further studies. According to Keller et al.,[2] the extended chains nucleate the growth of slender crystals in the direction of molecular orientation; the subsequent lamellar overgrowth produces stacks of oriented lamellae whose normals are parallel to the direction of molecular folding.

On the other hand, Keith[15] and Williamson[16] observed long intercrystalline links connecting two crystal planes. This result indicates the possibility of forming fibrous crystals from long chains under shear stress. Anderson[17] and Wunderlich[18] reported that molecular chains form fibrous crystallites under high pressure.

Recently, Hashimoto et al.[19,20] studied the morphology and the deformation mechanism of polyethylene films made by calendering from a stressed polymer melt. The morphology and deformation mechanism of the submicroscopic structure were studied by means of small-angle X-ray scattering, wide-angle X-ray diffraction, and electron microscopy.[19] Moreover, in a later paper,[20] a study using a higher molecular weight polymer (HMW2-L) was extended from the submicroscopic scale to the microscopic scale in order to investigate the superstructure of the lamellae by means of a polarizing microscope and light scattering. One of their purposes was to observe how the superstructure of the lamellae of these particular specimens may be reconciled with their X-ray and electron micrograph data and with the concept of row-nucleated cylindrites by Keller et al.[2] and other authors. According

0024-9297/80/2213-1187$01.00/0